Functional Effects of Glycosylation at Asn-579 of the Epidermal Growth Factor Receptor†

Kristin B. Whitson,‡,§ Stefanie R. Whitson,‡ Monica L. Red-Brewer,‡ Austin J. McCoy,§ Angela A. Vitali,|| Francesca Walker,⊥ Terrance G. Johns,|| Albert H. Beth,§ and James V. Staros*,‡,#

Department of Biological Sciences, Vanderbilt University, Nashville, Tennessee 37235, Department of Molecular Physiology and Biophysics, Vanderbilt University, School of Medicine, Nashville, Tennessee 37232, Ludwig Institute for Cancer Research, Oncogenic Signaling Laboratory, Austin Hospital, Heidelberg 3084, Australia, Ludwig Institute for Cancer Research, Epithelial Biochemistry Laboratory, Parkville, Victoria 3052, Australia, Department of Biochemistry and Cell Biology, State University of New York (SUNY)—Stony Brook, Stony Brook, New York 11794

Received April 23, 2005; Revised Manuscript Received August 30, 2005

ABSTRACT: We have investigated functional effects of glycosylation at N^{579} of the epidermal growth factor receptor (EGFR). Our previous study showed that the population of cell-surface expressed EGFRs in A431 cells, a human epidermoid carcinoma cell line, is composed of two subpopulations that differ by glycosylation at N^{579} [Zhen et al. (2003) *Biochemistry* 42, 5478−5492]. To characterize the subpopulation of receptors not glycosylated at N^{579}, we established a 32D cell line expressing a point mutant of the EGFR (N579Q), which cannot be glycosylated at this position. Analysis of epitope accessibility suggests that the lack of glycosylation at N^{579} weakens auto-inhibitory tether interactions, and cross-linking experiments suggest a somewhat elevated level of preformed N579Q-EGFR dimers in the absence of ligand relative to wild-type EGFR (WT-EGFR). However, ligand drives the majority of N579Q-EGFR dimerization, suggesting that untethering, while necessary, is not sufficient to drive dimerization. Ligand-binding experiments reveal a much greater fraction of N579Q-EGFRs in a high-affinity state compared to the fraction of WT-EGFRs in a high-affinity state. However, differences in the kinetic association and dissociation rates indicate that the high-affinity states of the WT and the N579Q receptors are distinct. EGF-stimulated phosphorylation in cells expressing N579Q-EGFRs results in notable differences in the pattern of tyrosine phosphorylated proteins compared with that obtained in cells expressing WT-EGFRs. Moreover, although WT-EGFRs confer cell survival in 32D cells in the absence of interleukin-3 and EGF, we found that receptors lacking glycosylation at N^{579} do not. This is the first study of which we are aware to show that selective glycosylation of a specific N-glycosylation site can produce two functionally distinct receptors.

Epidermal growth factor (EGF)[1] binds to and activates its cell-surface receptor [the EGF receptor (EGFR)]. Upon ligand binding, EGFRs homodimerize or heterodimerize with related receptors of the ErbB family, dependent upon tissue-specific expression patterns (*1*). Tyrosine kinase activity is concomitantly increased with dimerization (*2*), and downstream cellular signaling pathways are initiated that ultimately result in diverse effects, including mitogenesis and proliferation, cell survival, organogenesis, migration, or differentiation (*3*). The EGFR and other ErbB receptors have repeatedly been causally associated with tumor progression, and their overexpression has been correlated with poor prognosis (*4*, *5*).

Crystallographic studies of the extracellular ligand-binding domains of ErbB receptors in both liganded (*6*−*8*) and unliganded (*9*−*11*) forms reveal two distinctly different conformations of receptor ectodomains, providing insight into the mechanism of receptor activation by ligand. In what is interpreted to be the active conformation, ligand is bound by primary contacts with receptor subdomains I and III; a loop in subdomain II, termed the dimerization arm, interacts with the dimerization arm of the adjacent receptor of the receptor dimer. In contrast, in what is interpreted to be the inactive conformation, the dimerization arm interacts with a

† This work was supported by Grants R01 GM055056 (to A.H.B. and J.V.S.) from the National Institutes of Health and DAMD17-02-1-0608 (to K.B.W.) from the Department of Defense Congressionally Directed Medical Research Program Breast Cancer Initiative and in part by the National Health and Medical Research Council of Australia.

* To whom correspondence should be addressed. Telephone: 631-632-6976. Fax: 631-632-6900. E-mail: james.staros@stonybrook.edu.

‡ Department of Biological Sciences, Vanderbilt University.

§ Department of Molecular Physiology and Biophysics, Vanderbilt University.

|| Ludwig Institute for Cancer Research, Oncogenic Signaling Laboratory.

⊥ Ludwig Institute for Cancer Research, Epithelial Biochemistry Laboratory.

State University of New York (SUNY)—Stony Brook.

[1] Abbreviation: EGF, epidermal growth factor; EGFR, EGF receptor; WT, wild type; IL-3, interleukin-3; HPLC, high-performance liquid chromatography; CHO, Chinese hamster ovary; mEGF, murine EGF; FITC, fluorescein 5-isothiocyanate; F-EGF, fluorescein-labeled H22Y-mEGF; PCR, polymerase chain reaction; WCM, WEH1-3B-conditioned medium; FACS, fluorescence-activated cell sorting; SDS−PAGE, sodium dodecyl sulfate−polyacrylimide gel electrophoresis; BS^3, bis-(sulfo-*N*-succinimidyl)suberate; CMF-PBS, Ca^{2+}-free, Mg^{2+}-free phosphate-buffered saline; 7-AAD, 7-aminoactinomysin D; MAPK, mitogen-activated protein kinase.

10.1021/bi050751j CCC: $30.25
Published on Web 10/19/2005

Table 1: Canonical N-Glycosylation Site Usage in the EGFR Ectodomain Expressed in Different Cell Types

site	subdomain	A431[a]	CHO[b]	Sf9[c]
N^{104}	I	no	yes	nd[d]
N^{151}	I	yes	yes[e]	nd[d]
N^{172}	I	no	yes/no[e,f,g]	nd[d]
N^{328}	III	yes	yes[e,g]	yes
N^{337}	III	yes	yes[e]	yes
N^{389}	III	yes	yes	yes[h]
N^{420}	III	yes	yes[e]	yes
N^{504}	IV	yes	yes	yes
N^{544}	IV	yes	yes	yes
N^{579}	IV	partial (80%)	yes	yes
N^{599}	IV	yes	no	nd[d]

[a] Data from Zhen et al. (*18*). [b] Compiled data from Smith et al. (*21*) and Sato et al. (*20*). [c] Compiled data from structural studies of Ferguson et al. (*8*) and Li et al. (*11*). [d] Not described by either Ferguson et al. (*8*) or Li et al. (*11*). [e] Resolved in structural studies of Ogiso et al. (*6*). Both this construct and that used by Garrett et al. (*7*) were expressed in CHO-derived Lec8 cells. [f] Disagreement in the data from Smith et al. (*21*) and Sato et al. (*20*). [g] Resolved in structural studies of Garrett et al. (*7*). [h] Not resolved in structural studies of Ferguson et al. (*8*).

disulfide-bonded loop in subdomain IV termed the tether loop to form an autoinhibitory tether, both preventing the exposure of the dimerization arm and orienting subdomains I and III in a way that the ligand cannot simultaneously contact both. Modeling of the entire receptor ectodomain reveals that, in the untethered, active form, the tether loop might interact with the analogous tether loop of the dimer partner (*3*, *12*), suggesting the formation of an additional dimerization interface. In support, peptides modeled on the tether loop have been shown to disrupt ErbB dimerization (*13*).

The EGFR ectodomain is normally heavily N-glycosylated (*14*), with sugar moieties accounting for nearly 40 kDa of the 180 kDa mass (*15*). Oligosaccharides include both high-mannose and complex types (*14*). The biosynthesis of attached oligosaccharides has been investigated (*14*, *16*), and structural information is available for several of the oligosaccharide moieties (*14*, *17*, *18*). A total of 11 canonical glycosylation sites, specified by NXS/T (where X is any amino acid except proline) are encoded in the amino acid sequence of the extracytoplasmic ligand-binding domain of the receptor (*19*). In addition, one noncanonical site, N^{32}NC has been identified (*20*).

Glycosylation patterns *in vivo* are generally cell- and tissue-type specific. On the basis of crystallographic studies of soluble EGFR ectodomain (*6*−*8*, *11*) expressed in Chinese hamster ovary (CHO)-derived cell lines or Sf9 (insect) cells and crystallized without endoglycosidase treatment, all N-linked glycosylation sites are solvent-accessible. In addition, the first one or two sugar moieties of several oligosaccharides were well-resolved in these studies and one larger oligosaccharide was seen in one of the studies (*11*). A mass spectroscopic study of glycosylation-site usage in the EGFR expressed in A431 (human epidermoid carcinoma) cells revealed that 2 of the 11 canonical glycosylation sites are not glycosylated and that 8 sites are always glycosylated. However, the canonical site at N^{579} was shown to be glycosylated on only a fraction (80%) of receptors (Table 1) (*18*).

Glycosylation of the EGFR (reviewed in refs *22* and *23*) functions in its translocation and maturation (*16*, *24*). EGFRs synthesized in the presence of an inhibitor of N-linked glycosylation are devoid of ligand-binding and kinase activity (*14*). However, glycosylated EGFRs subjected to enzymatic removal of oligosaccharides retain the ability to bind ligand (*15*). Moreover, EGFR that contains only high-mannose-type attachments may differ in both ligand-binding affinity and downregulation from the receptor that also contains complex carbohydrates (*23*).

The functions of several specific N-glycans in EGFR have been investigated. Carbohydrate attachments are often found to influence local protein conformation near glycosylation sites (*25*), and it has been suggested that glycosylation of subdomain III sites may be necessary for proper receptor conformation and ligand-binding function (*26*). Mutations abolishing oligosaccharide attachment at N^{328}, N^{337}, and N^{389} showed no detectable effect on ligand-binding or kinase activity (*27*). On the other hand, a mutant receptor lacking the carbohydrate attachment at N^{420} did not bind ligand, spontaneously oligomerized, and was constitutively active (*27*). Moreover, glycosylation at N^{544} in subdomain IV may affect proper folding of subdomain III, because EGFR lacking the N-glycan was not recognized by the conformationally sensitive antibody C225 (*28*). The consequences of partial glycosylation at the noncanonical N^{32} site in subdomain I have also been investigated, but no functional difference between EGFR lacking the N-glycan at this site and that containing the N-glycan attachment was detected (*20*).

Two naturally occurring subpopulations of WT-EGFR that differ in glycosylation at N^{579} occur in at least one tumor cell line in which the EGFR is highly overexpressed (*18*), but the functional consequences of the lack of glycosylation at N^{579} have not been previously studied. Structurally, N^{579} is situated at the tip of the subdomain IV auto-inhibitory tether loop. Weaker interactions between subdomains II and IV both increase the affinity of EGFR for ligand (*8*, *29*) and result in a more conformationally flexible EGFR ectodomain by altering the kinetics of tethering and untethering (*29*). These observations raise the intriguing possibility that EGFRs that are not glycosylated at N^{579} may be a naturally occurring, functionally distinct class of receptors.

MATERIALS AND METHODS

Preparation of Fluorescein-Labeled H22Y-mEGF. Expression of H22Y-mEGF (murine EGF) was carried out using *Pichia pastoris* strain 204414 (American Tissue Type Collection). The H22Y-mEGF gene was amplified from the pinIII-ompA-H22Y-mEGF vector (*30*) using primers that contained appropriate restriction sites for insertion into the pic9k plasmid (Invitrogen). The resulting expression vector, containing the H22Y-mEGF gene flanked by *Sac*I and *Not*I restriction sites and the gene encoding resistance to kanamycin, was transformed into competent cells, and a high-expressing clone was selected by methods given by the manufacturer (Invitrogen). Briefly, transformants were initially streaked onto yeast extract peptone dextrose plates to allow vector integration but were selected by their ability to grow on regeneration dextrose medium devoid of histidine. Integration into the *P. pastoris* genome was confirmed by polymerase chain reaction analysis. Transformants were streaked onto minimal methanol plates and then restreaked onto plates containing a range of G418 concentrations. A

single colony grown in the presence of 1 mg/mL G418 was selected for screening by growth with methanol as the sole carbon source. Cells were inoculated into 10 mL of buffered glycerol complex medium and grown at 30 °C with shaking at 100 rpm. After 24 h, an OD_{600} of 5−10 was reached, and cells were pelleted by centrifugation at ∼1500*g* for 5 min at 4 °C. For large-scale production, 10 cultures (10 mL) were grown in buffered methanol complex medium for about 72 h. Each culture was supplemented with 0.3 mL of 50% methanol every 24 h. When the OD_{600} reached 62, cells were pelleted and the resulting supernate was processed to isolate H22Y-mEGF as previously described (*31*). The yield of H22Y-mEGF was typically 20 μg/mL. Labeling of H22Y-mEGF with fluorescein isothiocyanate (F-EGF) and subsequent purification proceeded as described in Wilkinson et al. (*32*).

Mutagenesis and Plasmid Construction. The N579Q-EGFR construct was generated by oligonucleotide-directed mutagenesis of pCER plasmid DNA (*30*), which contains the gene encoding WT-EGFR in the pCDNA3.1(−) expression vector (Invitrogen). The mutagenized PCR product contained appropriate bases for substitution of N^{579} with glutamine and silent mutations for insertion of a unique *Spe*I restriction site. The product was subcloned into the pCER construct using *Bsmb*I (confirmed as unique by restriction digest of the pCER construct) and *Cla*I restriction sites in the gene encoding EGFR and transformed into competent *Escherichia coli* DH5α cells. The construct was verified by restriction digest with *Spe*I and *Cla*I and DNA sequencing (Vanderbilt-Ingram Cancer Center DNA Sequencing Shared Resource, Vanderbilt University). The T581A mutation was produced using methods previously described (*33*).

Cell Culture. 32D clone 3 (American Type Culture Collection) and 32D-based cell lines were maintained in RPMI-1640 containing 15% fetal bovine serum and 5% WEH1-3B-conditioned medium [as a source of interleukin-3 (IL-3)] (WCM). Cells were grown, washed, and harvested as previously described (*31*). Cell density was determined either by counting with a hemocytometer, counting using a Coulter Z1 particle counter, or by spectrophotometry, where $OD_{600} = 0.5$ corresponds to 1.8×10^6 cells/mL (*32*).

Establishment of Clonal Cell Lines. Electroporation of parental 32D cells with pCER-N579Q-EGFR plasmid DNA and initial selection of N579Q-EGFR-expressing cells with G418 were carried out essentially as previously described (*32*). Cells that survived G418 selection were stained for EGFR expression by incubation with 10 μg/mL anti-EGFR mAb 528 (Santa Cruz Biotechnology) for 20 min on ice followed by similar incubation with 10 μg/mL FITC-conjugated goat anti-mouse IgG_{2a} (Southern Biotech). Clonal cell lines were established by fluorescence-activated cell sorting (FACS) as previously described (*34*) (Veterans Administration Medical Center, Flow Cytometry Laboratory, Nashville, TN).

EGFR cell-surface expression in cells containing the N579Q-EGFR gene was confirmed by comparison of fluorescence from stained cells with cells that were either unstained or that had been stained using a nonspecific IgG_{2a} as the primary antibody. When putative clonal cell populations reached sufficient density, cells were reanalyzed by flow cytometry as described below to determine the monoclonality of each population. N579Q-EGFR expression levels were initially estimated by comparing the linear mean fluorescence of each clonal population with an EGFR-expressing cell line (WT3), for which the number of receptors/cell has been previously determined (*30*). From this method, we established several monoclonal cell lines that express N579Q-EGFR. Cell lines that experienced reversion of receptor expression levels over several passages were resorted, where only a small fraction of cells with the highest expression levels were collected. Exponentially growing cell populations were expanded until a sufficient number of cells were obtained, and stocks were made by suspending cells at a density of 1×10^7 cells/mL in RPMI-1640/15% FBS/5% WCM/7.5% dimethyl sulfoxide. Frozen stocks were maintained in liquid nitrogen. Two clonal cell lines in particular were chosen for these studies, 2NQ.8.2 [which expresses a similar number of receptors as WT3 (∼80 000−100 000 receptors/cell)] and 3NQ [which has more than twice the number of receptors/cell as WT3 cells as assessed by flow cytometry, required for the stopped-flow fluorescence binding experiments (*35*)].

T581A-EGFR was expressed in either 32D cells as described for the N579Q-EGFR or 293T cells using our previously described approach (*33*).

Antibody Recognition of EGFR. Samples of either 32D parental cells, WT3 cells, T581A-EGFR cells, or 3NQ cells to be assessed for reactivity with conformation-dependent antibodies were stained and analyzed by flow cytometry with linear-range detection essentially as described in Walker et al. (*29*) and Ewald et al. (*36*). Cells were incubated for 20 min on ice with saturating doses of either 10 μg/mL mAb 528 (Santa Cruz Biotechnology or the Biological Production Facility at the Ludwig Institute for Cancer Research, Melbourne, Australia), mAb 806 (Biological Production Facility at the Ludwig Institute for Cancer Research), mAb C225 (the kind gift of Dr. Carlos Arteaga), Ab-11 (Neomarkers), or 15 nM F-EGF. Samples were subsequently incubated for 20 min on ice with 10 μg/mL secondary antibody [FITC-conjugated goat anti-mouse IgG (Becton Dickinson) or FITC-conjugated monoclonal mouse IgG_{2a} anti-human IgG_1 for mAb C225 (Sigma)]. Samples suspended in F-EGF were incubated in the dark on ice for at least 1 h (to allow equilibrium binding) prior to analysis. Collected data were smoothed, and the median fluorescence values and standard deviation of each histogram were determined. The ratio of the background-subtracted median fluorescence of 3NQ/WT3 cells incubated with F-EGF or each of the conformationally sensitive antibodies allowed for determination of the relative number of accessible binding sites. The error in each ratio was determined by error propagation of the standard deviations of the original histogram data. Scatchard analysis of T581A-EGFR with iodinated mAb 806 and 528 was performed as previously described (*37*).

Determination of Association and Dissociation Rates. The measurement of the real-time association kinetics of F-EGF to N579Q-EGFR in 3NQ cells was carried out by stopped-flow fluorescence spectroscopy as previously described for the measurement of F-EGF binding kinetics to WT-EGFR expressed in 32D cells (*32*, *34*, *35*). The excitation source used was a Melles Griot IMA 420 argon-ion laser. 3NQ cells were used at final cell densities of 7.6×10^6, 4.7×10^6, and 2.4×10^6 cells/mL, and ligand stocks were made by serial dilution and used at final concentrations of 1.0, 1.5, 2.0, 3.0, 5.0, 7.5, 10.0, and 15.0 nM. Cells were equilibrated,

and measurements were taken at 20 °C [preventing internalization of occupied receptors (*32*)]. Data were acquired at 38 ms intervals, and 10 consecutive mixing experiments were performed for each cell density and F-EGF concentration.

Methods for the measurement of F-EGF dissociation from intact cells by perturbation of equilibrium through dilution have been reported (*32*) and were repeated for 3NQ cells as described. The experimental instrumentation was modified by using a T-format spectrofluorimeter (Photon Technologies International) and associated software for detection purposes; however, the optics and excitation source were the same as for association experiments described herein and in Wilkinson and Staros (*34*). Cell suspensions at final densities of approximately 150×10^6 and 120×10^6 were equilibrated for 10 min with 150 nM F-EGF, then diluted either 25-, 50-, 75-, or 100-fold by hand mixing into the appropriate volume of buffer in a 1 cm^2 cuvette to a 1 mL final sample volume, and stirred with a small stir bar throughout the measurements. As in association experiments, instrument and reagent temperatures were maintained at 20 °C by a circulating water bath. Data were acquired at 100 ms intervals for 12 min. The approximate dead time for hand mixing was about 20 s. For each dilution experiment of a particular cell density and dilution factor, 8−10 consecutive mixing experiments were performed.

Data from each binding curve at a given F-EGF concentration and cell density were averaged to yield the final experimental data set. Each data set was corrected for the background signal because of cell autofluorescence and light scattering, and the vertically and horizontally polarized emission intensities were used to calculate the anisotropies according to formulas given in ref *32*. The data were analyzed with global fitting of the surface (*38*) using a two-independent receptor class model. Kinetic rates were described by

$$\frac{d[\text{F-EGF}_{\text{bound}}]}{dt} = [\text{F-EGF}_{\text{free}}](k_{\text{on1}}[\text{EGFR}_1] + k_{\text{on2}}[\text{EGFR}_2]) - (k_{\text{off1}}[\text{F-EGF}_{\text{bound1}}] + k_{\text{off2}}[\text{F-EGF}_{\text{bound2}}]) \quad (1)$$

where k_{on1} and k_{off1} are kinetic association and dissociation rates for one receptor class ($EGFR_1$) and k_{on2} and k_{off2} are the corresponding kinetic rates for the second class of receptors ($EGFR_2$). Observed anisotropy was calculated from the concentrations of the individual species using the formula

$$r_{\text{measured}} = r_{\text{free}}\left(\frac{[\text{F-EGF}_{\text{free}}]}{[\text{F-EGF}_{\text{total}}]}\right) + r_{\text{bound}}\left(\frac{[\text{F-EGF}_{\text{bound}}]}{[\text{F-EGF}_{\text{total}}]}\right) \quad (2)$$

where r_{free} is the anisotropy of F-EGF free in solution and r_{bound} is the anisotropy of F-EGF bound to receptors in cells. The differential rate equations were solved using the method of finite difference in a subroutine incorporated into the global analysis kernel (Globals Unlimited). The anisotropy of F-EGF free in solution was fit individually for each data set in the final global analysis. Error analysis of the fitting parameters was performed as previously described (*32*).

Dimerization Experiments. Cells expressing either WT-EGFRs (WT3) or N579Q-EGFRs (2NQ.8.2) were treated ±mEGF for 15 min, and samples were cross-linked with 1 mM bis(sulfo-*N*-succinimidyl)suberate (*39*) (BS^3, Pierce) for 30 min at 20 °C. The reaction was quenched by addition of 50 mM glycine at pH 7.4 for 5 min, and cell lysates were prepared as previously described (*30*, *36*). Sodium dodecyl sulfate−polyacrylimide gel electrophoresis (SDS−PAGE) was performed under reducing conditions with the NuPAGE Electrophoresis System (Invitrogen) according to instructions of the manufacturer, using a 4−12% gradient gel. The protein was transferred to nitrocellulose using the NuPAGE Electrophoresis System at 30 V for 2.5 h. Blots were blocked, probed, and visualized as previously reported (*36*, *40*) using 1005 rabbit polyclonal anti-EGFR (Santa Cruz Biotechnology) and horseradish peroxidase conjugated donkey anti-rabbit IgG (Santa Cruz Biotechnology). The films were subjected to densitometric analysis to determine the fraction of receptor dimers formed at each ligand concentration using a transmittance scanner and Corel Photopaint 11 software (Corel Corporation). Dose−response data were fit to a four-parameter logistic equation with a variable Hill slope using SigmaPlot 8.0 software (SPSS).

Immunoblot Analysis of Tyrosine Phosphorylation. A total of 6×10^6 32D, WT3, or 2NQ.8.2 cells were harvested, washed 3 times with Ca^{2+}-free, Mg^{2+}-free phosphate-buffered saline (CMF-PBS) to remove residual IL-3 and serum, and suspended in serum-free, IL-3-free RPMI-1640 medium. After incubation for 3−4 h at 37 °C, cells were treated ±17 nM (100 ng/mL) mEGF for 5 min at 37 °C. Samples were harvested and lysed in 250 μL of lysis buffer as previously described (*36*). The total protein concentration of each lysate was determined using a BCA protein concentration assay (Pierce) according to the instructions of the manufacturer. SDS−PAGE, transfer to nitrocellulose membranes, and Western blotting for EGFR were as described above. Membranes were stripped as previously described (*40*), blocked, and reprobed with primary (mAb pY99 mouse anti-phosphotyrosine IgG_{2b}, Santa Cruz Biotechnology) and secondary (horseradish peroxidase conjugated donkey anti-mouse IgG) antibodies.

Cell Growth and Viability Assays. Experiments were performed according to Ewald et al. (*36*) with the following modifications: 32D, WT3, and 2NQ.8.2 cells were initially suspended at a density of about 1×10^5 cells/mL in RPMI-1640 and 15% FBS ± either 5% WCM or 17 ng/mL EGF. At given time points, samples were removed and living cells were counted with a hemocytometer. Parallel samples at the same time points were stained with 2 μg/mL of 7-amino-actinomysin D (7-AAD, Molecular Probes) and analyzed by flow cytometry to determine the fraction of viable cells in the culture.

RESULTS

Receptor Expression and Preliminary Characterization. We constructed a mutant receptor in which N^{579} was replaced with Gln and expressed N579Q-EGFR in 32D cells. Monoclonal cell lines were selected for further studies based on flow cytometry and SDS−PAGE analyses, where chosen clones displayed monoclonal receptor expression at a level similar to that of a previously characterized WT-EGFR 32D cell line, WT3 (*30*), and had similar receptor mobility as WT-EGFR in SDS−PAGE under reducing conditions. Cell lines initially isolated by these methods exhibited decreased and variable receptor expression after several weeks in

culture; however, after multiple rounds of FACS sorting, cell lines were obtained that were appropriate for the experiments reported herein. Reversion of receptor expression levels over multiple passages was prevented by greatly expanding the sorted populations of exponentially growing cells and preparing numerous high-density frozen stocks. Monoclonality of cell stocks was ensured by flow cytometry analysis of samples of the cultures used to prepare frozen stocks, and for all experiments, stocks were thawed and cultured no more than 1 week prior to data collection.

Reactivity with Conformationally Sensitive Antibodies. To test whether the N579Q point mutation resulted in significant misfolding of the EGFR ectodomain, we performed a flow cytometry-based assay using conformationally specific reagents. Specifically, F-EGF recognizes the WT-EGFR ligand-binding pocket, and the monoclonal antibodies Ab-11, 528, C225 (Cetuximab), and 806 are directed to specific epitopes on the extracellular domain of the EGFR. While treatment with Ab-11 does not abrogate ligand binding by the receptor, both 528 and C225 have been shown to block ligand binding (*4*, *11*) through interaction with their subdomain III epitopes (*11*, *28*, *29*). The antigen-binding fragment of C225 has also been suggested to interact with the EGFR ectodomain so that the equilibrium of conformations in the population is driven toward a tethered, inactive receptor configuration (*11*). The epitope for 806 has been mapped (*28*, *33*) to a region near the junction of subdomains II and III and has been suggested to recognize a transitional, untethered form of the monomeric receptor (*28*, *29*, *33*).

Samples containing equal numbers of cells expressing either WT-EGFR or N579Q-EGFR were stained with each reagent, and the mean fluorescence was analyzed by flow cytometry. Assuming that F-EGF recognizes all correctly folded receptors at the cell surface, the proportion of EGFR reactive with each antibody can be determined by comparison of the relative fluorescence for each sample (Figure 1). 528 and Ab-11 (not shown) recognize both WT- and N579Q-EGFR comparably, strongly suggesting that the mutant receptor is properly folded and expressed at the cell surface. Under the saturation binding conditions of the experiment, the reactivity of C225 with cells expressing N579Q-EGFRs (3NQ) was slightly reduced compared with cells expressing WT-EGFR (WT3). However, 806 clearly recognizes cells expressing the N579Q-EGFR preferentially, with approximately 3-fold greater reactivity to N579Q-EGFR than to WT-EGFR across multiple experiments. Thus, the epitope for 806 is more often available in the unliganded N579Q-EGFR than WT-EGFR, consistent with a less frequently tethered conformation of this receptor.

To further confirm the role of glycosylation in the modulation of EGFR tethering, we constructed a second mutant where the same glycosylation motif was destroyed by changing the threonine at 581 to alanine (T581A). Because T^{581} does not interact with the tether interface at all (*8*), this mutation tests the remote possibility that effects seen for N579Q-EGFRs are the result of the change of the amino acid. As a measure of the relative untethering of this alternative glycosylation-negative variant, we determined the ratio of mAb 528 binding compared to that of mAb 806 binding by flow cytometry analysis in 32D cells and by flow cytometry and Scatchard analyses in 293T cells. When compared to mAb 528, mAb 806 showed increased binding to the T581A variant in both 32D and 293T cells as evidenced by an increase in the ratio (Table 2), suggesting that this variant also displays increased untethering. Further, Scatchard analysis with 293T cells clearly confirmed the

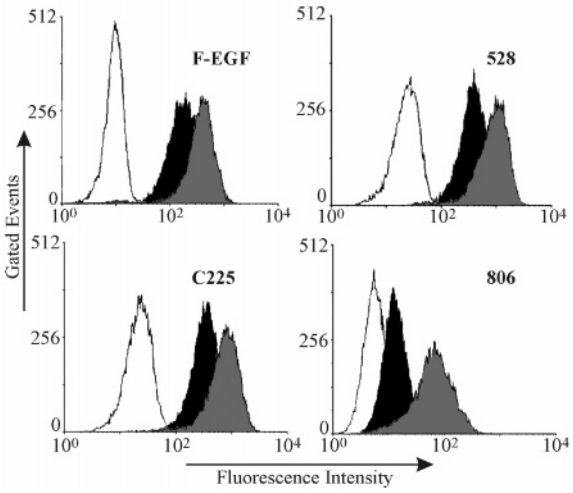

Background subtracted median fluorescence

	F-EGF	528	C225	806
32D	5±3	22±6	6±8	0±3
WT3	174±20	415±41	401±37	9±5
3NQ	415±47	992±93	851±80	67±14

3NQ:WT3 Ratio of the number of accessible binding sites

F-EGF	2.4±0.004
528	2.4±0.01
C225	2.1±0.004
806	7.4±2.6

FIGURE 1: Representative data set showing the binding of F-EGF and conformation-specific monoclonal antibodies with cells expressing WT-EGFR (WT3) or N579Q-EGFR (3NQ). Nonspecific binding was assessed by reactivity with the secondary antibody only or reactivity with nonexpressing parental 32D cells (white). To account for differences in receptor expression between N579Q-EGFR-expressing 3NQ cells (gray) and WT-EGFR-expressing WT3 cells (black), we compared the relative binding of F-EGF with the relative binding of three monoclonal antibodies. The 3NQ/WT3 ratio of binding for monoclonal antibodies 528 and C225 are essentially the same as the ratio for F-EGF; however, the 3NQ/WT3 ratio of binding of monoclonal antibody 806 is more than 3-fold higher. All reported errors were derived from the standard deviations of the original histogram data by error propagation. Analysis of data from this experiment and from separate experiments where data were normalized by 528 binding or Ab-11 binding yielded similar results.

Table 2: Binding Ratio of mAb 806/mAb 528 in Cells Expressing WT- or T581A-EGFRs[a]

	32D cells		293T cells	
	WT	T581A	WT	T581A
flow cytometry	0.030	0.159	0.208	0.335
Scatchard	nd	nd	0.049	0.146

[a] Stably transfected 32D or 293T cell lines were generated following transfection with the EGFR containing a T581A mutation that destroys the glycosylation motif for N^{579}. Cells were analyzed by flow cytometry using mAb 528 or mAb 806 as described in Figure 1, and the ratio of mAb 806/mAb 528 was determined. The 293T cell line was also analyzed by the method of Scatchard using iodinated antibodies to quantitatively determine the relative number of binding sites for each antibody. Replicate experiments produced similar results. nd = not determined.

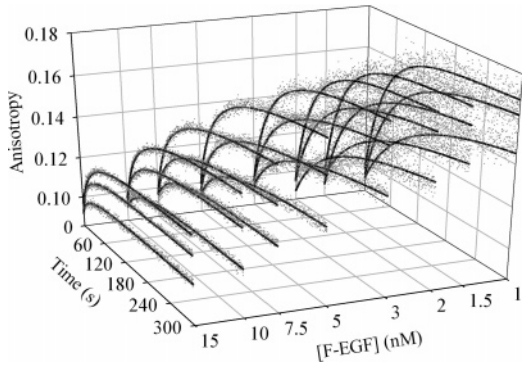

FIGURE 2: Real-time association of F-EGF with N579Q-EGFRs in intact 3NQ cells. Each mixing experiment yielded 7929 data points (with each point being the average of 8−10 experiments), and every 10th averaged point is plotted. Data points are displayed as a running average over five consecutive points to facilitate visualization. The recovered fit values of the receptor concentration in the association experiments (±1 standard deviation) were 6.6 (6.3−6.9) nM, 4.0 (3.9−4.2) nM, and 2.0 (1.9−2.1) nM. The fit lines represent the results of fitting a combined data surface that included association and dissociation experiments (Figure 3) to the two-independent receptor-class model. Parameter values recovered from this analysis are shown in Table 3.

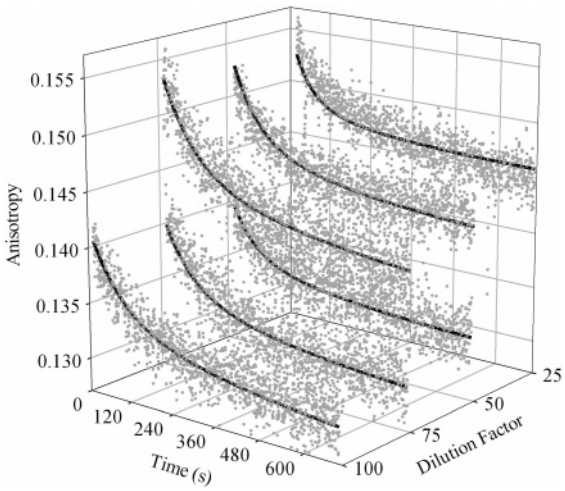

FIGURE 3: Dilution dissociation of F-EGF from N579Q-EGFR in 3NQ cells. For each given curve, a saturating concentration of F-EGF (150 nM) was equilibrated with a given suspension of cells expressing the receptor, where the recovered fit values for receptor concentration (±1 standard deviation) were 106 (91−120) nM and 84 (67−99) nM. These suspensions were mixed with buffer to give final dilutions of 25-, 50-, 75-, or 100-fold. For each dilution, 8−10 consecutive experiments were performed and the data were averaged. To facilitate visualization, data are plotted as the running average over 10 points with every fifth data point displayed. The fit lines represent the results of the global fit from the combined data surface (231 072 averaged data points; approximately 2×10^6 raw data points), including the 6 averaged curves from this experiment and 24 averaged curves in the association experiment (Figure 2) to the two-independent receptor-class model. The parameters recovered from this analysis are shown in Table 3.

increased binding of mAb 806 to the T581A-EGFR. In these experiments, the affinity of mAb 806 was approximately 3-fold greater for T581A-EGFR than for WT-EGFR (with equilibrium dissociation constants of 2.95×10^{-7} and 9.7×10^{-7} M, respectively). Therefore, a second independent glycosylation mutant shows increased untethering in two different cell lines, supporting the notion that glycosylation at N^{579} stabilizes the tethered form of the EGFR.

Measurement of Binding and Dissociation Rates of F-EGF with N579Q-EGFRs. A series of fluorescence experiments using F-EGF and N579Q-EGFR-expressing cells were performed to measure the kinetic association and dissociation rates of the ligand with the receptor in living cells. Rates of association of the ligand with the receptor were measured by monitoring the change in the anisotropy of the fluorescent ligand as a function of time after F-EGF was rapidly mixed with a suspension of cells. The measured anisotropy at each time point is a linear combination of the anisotropies of ligand free in solution and ligand bound to receptors. Low values of anisotropy are indicative of F-EGF that has high rotational mobility (free in solution); high values of anisotropy result from decreased rotational mobility of F-EGF (bound to EGFR in cells). The measured anisotropy approaches the value obtained at equilibrium over time. Performing experiments at multiple concentrations of ligand and receptor and globally fitting the data surface to the same parameters allow for the determination of well-defined constants for each kinetic parameter.

A total of 24 binding curves resulted from experiments that used eight concentrations of F-EGF (1.0, 1.5, 2.0, 3.0, 5.0, 7.5, 10.0, and 15.0 nM) and three cell densities (7.6×10^6, 4.7×10^6, and 2.4×10^6 cells/mL). These cell densities were calculated to yield receptor concentrations in the low nanomolar range; consequently, stoichiometric and substoichiometric ratios of ligand/receptor were achieved with the range of ligand concentrations used in these experiments. Anisotropies for each data set were calculated from background-corrected polarized emission intensities, resulting in the data surface shown in Figure 2. Each data set reveals a binding interaction that occurs on a time scale of seconds to minutes, similar to that of F-EGF/WT-EGFR binding in 32D cells (*32*, *34*). For a given cell density, substoichiometric concentrations of F-EGF have the highest terminal anisotropy and high F-EGF concentrations exhibit a lower value for the terminal anisotropy as a result of excess ligand in solution. As the receptor concentration decreases for a given ligand concentration, F-EGF equilibrium anisotropy also decreases, reflecting a higher ratio of unbound/bound F-EGF.

Association experiments allow for the determination of both association and dissociation rate constants; however, dissociation rates are better defined by directly measuring dissociation. Therefore, we performed dissociation experiments by perturbation of equilibrium through dilution. In these experiments, N579Q-EGFR-expressing cells were equilibrated with F-EGF under conditions in which the large majority of F-EGF was bound. Under these conditions, dilution of the cell suspension results in the dissociation of F-EGF from the receptor as the system re-equilibrates. After equilibration at 20 °C, cell/F-EGF suspensions were diluted 25-, 50-, 75-, or 100-fold and F-EGF dissociation was observed by monitoring changes in ligand anisotropy with time (Figure 3). The resulting data show a decrease in anisotropy for each curve, consistent with ligand dissociation as a result of re-equilibration, with greater dilutions resulting in larger changes in anisotropy.

To compare directly recovered kinetic parameters for N579Q-EGFR with previously reported stopped-flow kinetic binding parameters of F-EGF binding to WT-EGFRs in 32D cells, our data surface was fit by global analysis to the two-independent receptor class model. The results of this analysis

Table 3: Recovered Parameters from Global Analysis of the Association/Dissociation Data Surface to a Two-Independent Receptor Class Model for N579Q-EGFR Expressing Cells, WT-EGFR Expressing Cells, and Cells that Express Equal Amounts of WT-EGFR with ErbB2[a]

parameter	N579Q-EGFR	WT-EGFR[b]	WT-EGFR/ErbB2[c]
k_{on1} ($\times 10^6$ M^{-1} s^{-1})	2.1 (1.6, 2.5)	8.6 (5.6, 12.7)	3.1 (3.06, 3.19)
k_{off1} ($\times 10^{-3}$ s^{-1})	0.44 (0.03, 1.1)	1.7 (nd[d], 3.6)	0.9 (0.67, 0.98)
K_{D1} (nM)[e]	0.21 (0.02, 0.44)	0.20 (nd[d], 0.3)	0.27 (0.22, 0.31)
$\%R_1$[f]	69 (52, 83)	12.6 (7.5, 33.0)	96.6 (92.7, 98.0)
k_{on2} ($\times 10^6$ M^{-1} s^{-1})	7.4 (5.4, 10.7)	2.4 (2.01, 2.54)	6.0 (3.40, 16.3)
k_{off2} ($\times 10^{-3}$ s^{-1})	4.8 (3.1, 7.5)	2.1 (1.64, 2.36)	12 (10, 13)
K_{D2} (nM)[e]	0.65 (0.57, 0.70)	0.88 (0.82, 0.93)	2.1 (0.79, 2.9)
$\%R_2$[f]	31 (17, 48)	87.4 (67.0, 92.5)	3.4 (2.0, 7.3)

[a] Errors for recovered parameters are given in parentheses (±1 standard deviation). [b] Values as reported in Wilkinson et al. (*32*) for F-EGF binding to WT-EGFRs expressed in 32D cells. [c] Values as reported in Wilkinson and Staros (*34*) for F-EGF binding to WT-EGFR in EGFR/ErbB2 coexpressing 32D cells. [d] nd = not determined. [e] The K_D values were calculated where $K_{D1} = k_{off1}/k_{on1}$ and $K_{D2} = k_{off2}/k_{on2}$. [f] Fraction of total receptors associated with k_{on1} and k_{off1}, with the remaining fraction of receptors associated with k_{on2} and k_{off2}.

and the comparison with binding to WT-EGFRs (*32*) and WT-EGFRs when coexpressed with ErbB2 (*34*) are shown in Table 3. While the two-independent receptor-class model does not provide a perfectly accurate description of our data, it does provide a significantly better fit than a single receptor-class model (data not shown) as assessed by the fit variance. Further, analysis in the context of the two-independent receptor-class model allows direct comparison with numerous two-site analyses in the literature.

Global analysis of the association and dissociation data recovered parameters for the anisotropy of F-EGF bound to N579Q-EGFR (r_{bound}), the effective receptor concentration at each cell density, the rates of ligand association with (k_{on1} and k_{on2}) and dissociation from (k_{off1} and k_{off2}) the receptor, and the fraction of receptors in each receptor class (Table 3). The recovered value for r_{bound} (±1 standard deviation) obtained was 0.177 (0.174, 0.180), consistent with previously reported values (*32*, *34*). The value for the free anisotropy was allowed to float for each curve but was consistent with the previously reported value of 0.095 for all curves, never deviating more than 0.003 from this value. In fitting the data surface to the two-independent receptor-class model, no assumptions were made about the combination of rate constants required to describe each affinity class (such as constraining a high-affinity class to slow dissociation and fast association rate constants). Therefore, the rate constants that describe each receptor class were determined independently.

Ligand-Induced Activation of N579Q-EGFR. As a direct measure of N579Q-EGFR oligomerization, cross-linking studies using 32D cells expressing either WT-EGFR or N579Q-EGFR were performed. Intact cells were treated ± a saturating dose of mEGF, and cell-surface-expressed receptor dimers were trapped by cross-linking (*39*). Because the cross-linking experiment was carried out on intact cells and employed a membrane-impermeant cross-linking reagent (*39*), only those receptors exposed on the cell surface are cross-linked. It is highly unlikely that misfolded, aggregated receptors would be transported to the cell surface. Detection of receptors separated by SDS−PAGE was achieved by immunoblotting with an antibody specific for residues in the EGFR C-terminal tail. The results of these experiments (Figure 4A) show that although a fraction of receptors can be cross-linked to dimers in the absence of EGF, ligand binding drives dimerization of N579Q-EGFR and WT-EGFR similarly.

A more detailed analysis of dimer formation in response to increasing concentrations of mEGF revealed that the

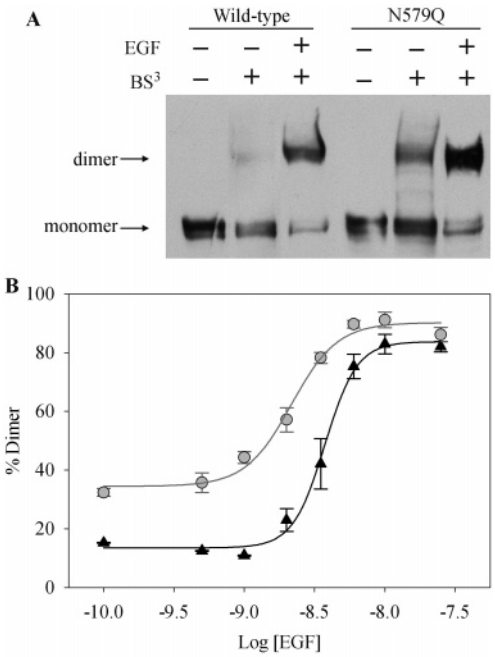

FIGURE 4: Ligand-induced dimerization of cell-surfaced expressed receptors in WT3 and 2NQ.8.2 cells. (A) Cells expressing WT- or N579Q-EGFRs were treated ±mEGF (25 nM final concentration) and ±BS^3 (1 mM final concentration) prior to lysis. (B) Cells were incubated in the presence of 0.1, 0.5, 1, 2, 3.5, 6, 10, or 25 nM mEGF (final concentrations), and receptor dimers were trapped by cross-linking with BS^3. This range of ligand concentrations corresponds to 1−97% receptor occupancy for both N579Q-EGFR (~3 nM) and WT-EGFR (~5 nM) based on ligand-binding constants. Samples were separated by SDS−PAGE, and the mono- and dimeric receptor species were quantified as described in the Materials and Methods. Presented curves for N579Q-EGFR (gray circles) and WT-EGFR (black triangles) are representative data from concurrent experiments, where the error bars represent error propagation of the standard deviation of the background.

proportion of N579Q-EGFRs that can be cross-linked to dimers in the absence of the ligand is greater than that for WT-EGFR (Figure 4B). While the absolute fraction of receptors that could be trapped in preformed dimers varied across multiple experiments because of variable cross-linking efficiencies under different conditions, the proportion of preformed dimers was consistently greater for N579Q-EGFR than for WT-EGFR, even though receptor expression in 2NQ.8.2 cells was less than in WT3 cells.

Ligand-induced dimerization of EGFR is thought to play a key role in activating the catalytic tyrosine kinase domain of the receptors, resulting in autophosphorylation and phos-

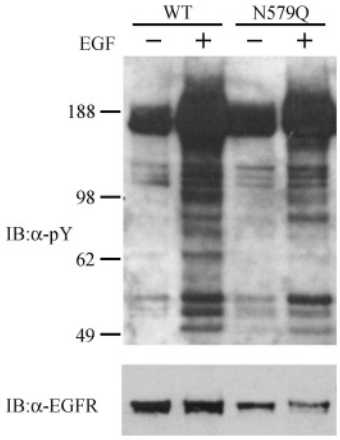

FIGURE 5: Ligand-induced stimulation of N579Q-EGFR kinase activity in 2NQ.8.2 cells. The parental 32D cell line (not shown), WT3 cells expressing WT-EGFR, or cells expressing N579Q-EGFR were incubated in the presence or absence of the activating ligand. Detection of EGFR and phosphotyrosine residues was achieved by immunoblotting with mAb 1005 and mAb pY99, respectively. Molecular mass standards (left) are expressed in kilodaltons.

phorylation of intracellular substrates. Cells expressing N579Q-EGFRs were starved of both serum and IL-3 and were then treated with mEGF. Lysates prepared from these cells were subjected to SDS−PAGE and were immunoblotted with an antibody against phosphotyrosines. The results of these experiments (Figure 5) reveal that, similar to WT-EGFR populations, ligand induces autophosphorylation of N579Q-EGFR. When the level of phosphorylation (α-pY) is normalized to the amount of receptor in each sample (α-EGFR), the fraction of N579Q-EGFRs that are phosphorylated in the absence of ligand is greater than that for WT-EGFR, consistent with a subtly higher proportion of receptors in preformed dimers. In addition, mEGF stimulates tyrosine phosphorylation of other cellular substrates in cells expressing N579Q-EGFR. Although the same downstream proteins appear to be phosphorylated in response to EGF, the extent of phosphorylation on some proteins appears different in N579Q-EGFR-expressing cells than in WT-EGFR-expressing cells.

Growth and Viability of N579Q-EGFR-Expressing Cells. 32D cells are normally dependent upon IL-3 for growth; however, in 32D cells that express WT-EGFRs, EGF stimulates growth in the absence of IL-3 (*36*). We tested whether N579Q-EGFR-expressing 32D cells also exhibit IL-3 independent growth by seeding cultures of cells in media containing serum and EGF but no IL-3. As expected, cells expressing N579Q-EGFRs grew under the same conditions as cells expressing WT-EGFRs (parts D−F of Figure 6). In addition, in cell lines with higher N579Q-EGFR expression (>100 000 receptors/cell), growth was slowed or arrested upon addition of EGF in comparison to a control sample that contained IL-3 but no EGF (data not shown). This phenomenon is similar to that observed when the same experiment is performed with 32D cells expressing higher levels of WT-EGFR (data not shown) and consistent with the observation of cell cycle arrest in response to EGF in cell lines in which the EGFR is highly expressed, such as A431 cells (*41*).

32D cells also require IL-3 for survival; however, it has been previously observed that 32D cells expressing WT-EGFR are able to survive in the absence of IL-3 if serum is

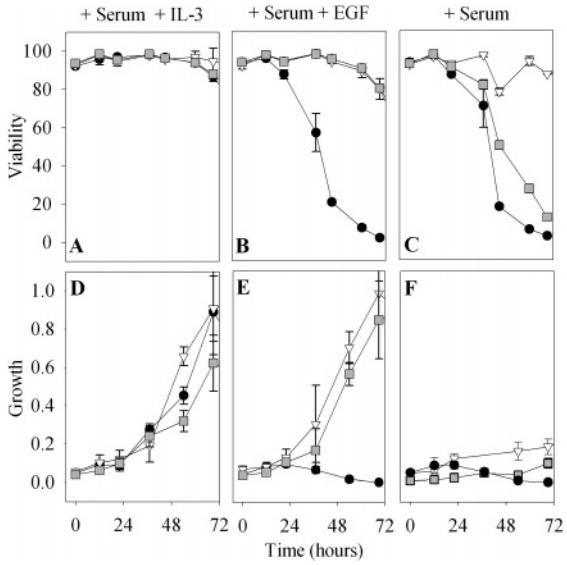

FIGURE 6: Viability and growth of parental 32D cells (black circles), WT-EGFR-expressing WT3 cells (white triangles), and N579Q-EGFR-expressing 2NQ.8.2 cells (gray squares). Each data point is the average of three identically treated samples, and the error bars represent 1 standard deviation. Results are representative of three independent experiments and were reproduced using other EGFR- and N579Q-EGFR-expressing clonal cell lines. Viability is expressed as the percentage of cells in each sample that did not take up 7-AAD. Growth of all samples was assessed by counting living cells in the culture and was normalized to the saturation density of WT-EGFR-expressing cells in the presence of serum and IL-3 (3×10^6 cells/mL).

present (*36*). To determine whether the N579Q-EGFR also confers IL-3-independent survival of 32D cells in the presence of serum, we performed further growth and viability studies in which cells were washed free of IL-3 and resuspended in a medium containing serum but no IL-3 or EGF (parts C and F of Figure 6). Samples of each cell line under each set of conditions were collected at 12 h intervals, stained with 7-AAD, and analyzed by flow cytometry to measure the fraction of the total cell population that remained viable. As shown previously (*36*), parental 32D cells exhibited decreasing viability over time, independent of the presence of serum, and WT-EGFR expressing cells remained viable in the presence of serum. However, in contrast to cells that express WT-EGFR, N579Q-EGFR-expressing cells do not remain viable in the absence of IL-3. This effect was reproducible over several experiments and multiple clonal populations of cells, suggesting that the effect is not specific to individual clones.

DISCUSSION

To study the native subpopulation of receptors not glycosylated at N^{579} in A431 cells, we made a conservative Asn to Gln mutation at residue 579, which prevents addition of oligosaccharide moieties to this residue while retaining the chemical character of the side chain, and expressed the N579Q-EGFR in 32D cells. 32D cells are a hematopoietic cell line that is devoid of endogenous ErbB receptors and does not secrete EGF family ligands, making it ideal for biochemical characterization of the receptors (*42*, *43*). In addition, these cells survive rapid stopped-flow mixing, enabling determination of the kinetic rates of ligand/receptor association and dissociation in living cells (*32*). Although

we have not explicitly determined the fraction of EGFR not glycosylated on N^{579} in this cell line, the differences observed between the N579Q-EGFR cell lines and 32D cells expressing WT-EGFR indicate that most if not all of the WT-EGFR population is glycosylated at N^{579} in these cells.

Conformation of Unactivated N579Q-EGFRs. It has been estimated that in the absence of ligand a large fraction (80−97%) of receptors in WT-EGFR populations are in a tethered configuration mediated by interactions between the subdomain IV tether loop and the subdomain II dimerization arm (*8*). Measurements of the equilibrium dissociation constant (K_D) for ligand binding to the soluble extracellular domain (*8*, *11*) or to cell-surface-expressed EGFRs with mutant tethers (*29*, *44*) support the hypothesis that interdomain hydrogen bonds between amino acid residues contribute to stabilization of the tether (*8*). The position of N^{579} at the tip of the tether loop offers the intriguing possibility that the oligosaccharide attached at this residue may also contribute to tether stability.

In general, glycan attachments are frequently located at regions of local protein secondary structure transition, such as when bound to an Asn residue at a β-hairpin turn, and addition of the carbohydrate may result in an increase in the rigidity of the local protein conformation (*45*). Protein/carbohydrate steric and hydrophilic/hydrophobic interactions most often occur with the first and second sugar rings, with the remainder of the oligosaccharide being flexible (*46*). Two determined crystal structures reveal the first core sugars of the oligosaccharide at N^{579}. The first core sugar of the N^{579} glycan attachment was ordered in the structure determined by Ferguson et al. (*8*). This structure suggests that the sugar ring is close enough in proximity to N^{256} and E^{258} in the subdomain II dimerization arm for hydrogen-bond formation. In the structure determined by Li et al. (*11*) with the antigen-binding fragment of C225 bound, the resolved sugar rings at N^{579} are directed farther away from the interface. The two available structures of the tethered receptor exhibit two of what are likely to be many conformers of the first sugar(s) of the oligosaccharide bound to N579. Stabilization of the tether by the oligosaccharide would not require a single static conformation. If, as the oligosaccharide samples the available conformational space, it makes significant contacts with the dimerization arm, it could significantly affect the activation energy for untethering and therefore the rate of untethering.

Our studies with conformation-specific antibodies under saturating conditions revealed a significant difference in exposure of the epitope for mAb 806 between receptors lacking glycosylation at N^{579} and WT-EGFR populations but only a slight difference in exposure of the epitope for C225. Previous studies have shown that mAb 806 recognizes an untethered form of the WT-EGFR (*28*, *29*, *33*). For comparison, the ΔCR1 mutant, which lacks the dimerization arm and therefore can assume neither the tethered nor the dimeric conformation, binds approximately 10-fold more mAb 806 than WT-EGFR (*29*). Any mutant that reduces tethering but can still dimerize, such as N579Q, would be expected to bind mAb 806 more than WT-EGFR but less than ΔCR1. Our data strongly correlate with the reactivity of mAb 806 with mutant receptors specifically designed to weaken protein−protein interactions in the autoinhibitory tether (V583D and D563H) or that are both tether- and dimerization-impaired (Y^{246} mutants) (*29*), suggesting that in the absence of ligand, EGFRs lacking the oligosaccharide at N^{579} are more often found in an untethered configuration.

While mAb 806 has been reported not to recognize WT-EGFRs expressed in epithelial cell lines (*29*), our studies revealed that this antibody binds to a small fraction of WT-EGFRs in 32D cells, an effect similar to that observed for WT-EGFRs in BaF/3 cells (*29*). Moreover, a fraction of WT-EGFR populations in cells that overexpress the receptor (*47*, *48*) is recognized by mAb 806, including about 10% of EGFRs expressed in A431 cells (*37*). These data support the hypothesis that interactions of the oligosaccharide moiety at N^{579} serve to strengthen the autoinhibitory tether. Removal of the N^{579} oligosaccharide likely reduces the energy of activation for transition between the tethered and untethered conformations.

Ligand Binding. EGF ligand/receptor interactions have been investigated for 30 years, and evidence for multiple affinity states of the receptor has been presented by many laboratories. Observation that a subsaturating dose of EGF resulted in maximal stimulation of the receptor (*49*) led to the original proposal for a high-affinity state, and equilibrium binding studies using a number of different cell types analyzed by the Scatchard method produce curvilinear plots suggestive of multiple affinity states (*50*). Although the presence of other ErbB receptors can modulate EGFR ligand-binding affinity (*34*), multiple affinity states are an intrinsic property of the receptor itself, because ligand binding to EGFR expressed in cells devoid of other ErbB receptors is best described by at least two affinity states (*30*, *32*). Most often, EGF ligand/receptor interactions have been described in the context of two independent receptor classes characterized by high- and low-affinity binding. To extend analysis of ligand association and dissociation rates to N579Q-EGFR and provide a comparison with previously reported kinetic parameters, we also fit and interpreted our data in the context of this model.[2]

A comparison of WT- and N579Q-EGFR ligand-binding kinetics (Table 3) suggests that the oligosaccharide moiety at N^{579} does play an important role in modulating ligand binding. The fraction of N579Q receptors that exhibit high-affinity binding (69%) is significantly higher than the high-affinity fraction of WT-EGFRs (12%) (*32*). In the context of the above antibody reactivity data, our kinetic data support the conclusion that the tethered conformation of the receptor is more favored in receptors glycosylated at N^{579} than in those which are not. These results are also consistent with previously reported experiments using receptors with mutations designed to weaken the interdomain tether through disruption of hydrogen-bond formation (V583D), which resulted in an increase in the observed high-affinity population from 3 to 12% (*29*). Another mutant designed to have a weakened tether interaction, H566F, also appeared to have a decreased rate of ligand dissociation; however, this experiment was performed using only a single concentration of ligand and receptor and fit to a single dissociation rate (*44*); therefore, it is difficult to compare with our data.

[2] Our previous studies have shown that K_D values that are calculated from kinetic data (*30*) differ from the values obtained by equilibrium measurements (*32*), even when the same fluorescent ligand is employed and the EGF receptor is expressed in the same cell type. We attribute this difference to limitations in the two-independent site model in which the data are analyzed (*30*).

Although the calculated equilibrium dissociation constants (K_D) for WT-EGFR and N579Q-EGFR are similar, differences in the kinetic rates of ligand association and dissociation indicate that the two affinity classes observed for N579Q-EGFRs are fundamentally different from those observed for WT-EGFRs. While ligand dissociates from N579Q-EGFR populations at two distinctly different rates (k_{off1} and k_{off2}), dissociation from WT-EGFR occurs at essentially one rate, accounting for statistical overlap in the measured parameters. Thus, in the WT-EGFR population, the high-affinity class is defined by a faster rate of ligand capture (k_{on1}) than the low-affinity class. In contrast, the high-affinity class of the N579Q-EGFR is characterized by a very slow rate of ligand release (k_{off1}). This switch in the character of high-affinity binding sites from one dominated by a fast on rate in WT-EGFRs to one dominated by a slow off rate in N579Q-EGFRs parallels our previous observation of a similar switch in states when WT-EGFR is expressed in the presence of ErbB2 (Table 3 and ref *34*). These distinctly different kinetic states most likely reflect different conformational states of the receptor. These results accentuate the importance of measuring kinetic association and dissociation rates to describe accurately ligand/receptor interactions.

The proposed conformational model of ligand binding (*8*, *12*) is consistent with kinetic data describing the interaction of EGF with N579Q-EGFR and with WT-EGFR in the presence of ErbB2, where the high-affinity state is defined by a slow off rate, consistent with bidentate ligand binding. However, it is not consistent with WT-EGFR expressed alone where the high-affinity state is defined by a fast on rate. Neither does the two-independent receptor class model sufficiently describe all states and conformations of WT-EGFR populations that interact with ligand nor does it provide an exact fit to experimentally observed data (*30*, *51*, *52*). Our data suggest that, at least in A431 cells, the WT-EGFR population may be described by no fewer than four receptor classes: two affinity states with or without oligosaccharide at N^{579}. Multiple conformational states are consistent with electron paramagnetic resonance data, suggesting at least two distinct conformations of the ligand-bound receptor (*53*).

Dimerization and Activation of N579Q-EGFR. It has been proposed that the accumulation of EGFR in an untethered conformation directly results in receptor dimerization (*8*, *12*), suggesting that N579Q-EGFRs might exist largely as preformed dimers, independent of the presence of ligand. While exposure of the subdomain II dimerization arm is necessary for the formation of dimeric complexes (*6*, *7*), it is apparently not sufficient in itself to drive dimerization, because in the absence of ligand, the expressed EGFR ectodomain containing only subdomains I−III does not detectably dimerize (*7*, *54*). Thus, the exposure of different elements or the formation of additional interactions induced by ligand binding are required to drive EGFRs into active dimers.

Although our cross-linking studies to measure receptor oligomerization of N579Q or WT-EGFR populations detected a greater proportion of N579Q-EGFR dimers than WT-EGFR populations in the absence of ligand, a comparable proportion of dimers were detected in the presence of saturating ligand. Furthermore, increasing condentrations of ligand drive dimer formation of N579Q-EGFR similarly to WT-EGFR. This suggests that the energy barrier between the untethered and dimerized conformations of the unliganded receptor is significant, so that mere exposure of the dimerization arm is insufficient for formation of functional dimers. In addition, the conformation of the cross-linkable complex formed in the absence of ligand may be slightly different than that of the ligand-induced dimer complex; it is possible that removal of the oligosaccharide at N^{579} perturbs an additional proposed dimer interface formed between the tether loops of adjacent receptor dimer partners (*12*). Studies of a Δ560−590 EGFR mutant (where the entire tether loop was removed) displayed delayed kinetics of ligand-induced receptor phosphorylation and phosphorylation of downstream-signaling molecules MAPK and Akt (*44*), perhaps indicative of disrupted dimerization kinetics.

Differences in association and dissociation rates of ligands with the EGFR have been shown to correlate with differences in the potency of mitogenic signaling effected by those ligands (*55*). In the active signaling complex, N579Q-EGFR is most likely similar to WT-EGFR in the initiation and activation of downstream-signaling cascades. However, because N579Q-EGFRs differ from WT-EGFR populations in their kinetic ligand-binding rates, it is possible that differential signaling may occur. D563H and V583D receptor mutants with weakened auto-inhibitory tethers studied by Walker et al. (*29*) activated MAPK and stimulated DNA synthesis at lower concentrations of ligand than WT-EGFR. Examination of the basal and EGF-dependent tyrosine phosphorylation of N579Q-EGFR (Figure 5) revealed an increase in phosphotyrosine content of N579Q-EGFR with the addition of ligand, consistent with ligand-induced receptor dimerization, and higher basal activity than WT-EGFRs, consistent with the greater fraction of preformed dimers observed.

Growth and Viability of N579Q-EGFR-Expressing Cells. To test whether there are discernible differences between WT-EGFRs and N579Q-EGFRs in their ability to signal for growth and survival, we performed viability and proliferation assays using 32D cells that expressed either WT- or N579Q-EGFR. Cell lines that expressed $\sim 10^5$ receptors/cell (WT3 and 2NQ.8.2) were used to avoid complications of spontaneous EGFR activation. Our results showed that addition of subsaturating or saturating doses of EGF to cells expressing physiological levels of the receptor relieved the normal IL-3 dependency for growth in 32D cells, resulting in cellular proliferation whether the EGF receptor expressed is WT or N579Q. Surprisingly, a key distinction between N579Q-EGFR- and WT-EGFR-expressing cells was found in the absence of the activating ligand. Consistent with previous observations (*36*), cells expressing WT-EGFR exhibit IL-3-independent survival in the presence of serum. However, cells expressing N579Q-EGFR do not survive under the same conditions, suggesting that lack of glycosylation at N^{579} of the EGFR can modulate cell-signaling pathways that support survival.

We previously reported a difference in the ability of two kinase-impaired mutants of EGFR to support cell survival in the absence of EGF, K721R-EGFR but not D813A-EGFR supporting survival in the absence of IL-3 but presence of serum (Table 4) (*36*). These two kinase-negative mutants likely differ subtly in the conformation of the ATP-binding pocket (*36*, *56*), and it is possible that this subtle difference in conformation mediates the observed difference in anti-

Table 4: Growth Properties of 32D Cells Expressing Wild-Type and Mutant Receptors from Data Presented in This Study and in Ewald et al. (*36*)[a]

	WT	N579Q	K721R	D813A
proliferation	yes	yes	no	no
viability	survive	die	survive	die

[a] Viability of cells is in media containing serum only, and proliferative properties are indicative of receptors having kinase activity that promotes cell proliferation with the addition of EGF in the absence of IL-3 and presence of serum.

apoptotic activity, perhaps through differences in recognition by downstream-signaling molecules. Any connection between the lack of glycosylation at N^{579} and conformational change in the kinase active site has yet to be discovered.

In conclusion, selective glycosylation at N^{579} of EGFR results in two naturally occurring subpopulations that are functionally distinct. The glycosylated and unglyscosylated subpopulations of EGFR differ both in the conformations of their ectodomains, with receptors lacking the oligosaccharide at N^{579} being more conformationally flexible, and in their ligand-binding properties, with a much greater proportion of these receptors binding ligand with high-affinity than in WT-EGFR populations. Moreover, the high-affinity state of the unglycosylated receptor is kinetically and likely conformationally distinct from that of the glycosylated receptor. In contrast to a previous report suggesting that disruption of the auto-inhibitory tether at the protein interface has little effect (*44*), we observe a greater fraction of preformed dimers and basal receptor phosphorylation in the absence of ligand for receptors lacking glycosylation at N^{579}, suggesting that glycosylation at N^{579} may be an important determinant of tether affinity. Finally, differences observed in EGF-induced phosphorylation of cellular proteins and in anti-apoptotic activity suggest that EGFRs glycosylated at N^{579} differ in downstream signaling from those not glycosylated at N^{579}.

ACKNOWLEDGMENT

We thank Dr. C. Guyer, the late Deirdre Dobbins-Sanchez, and M. Coco for assistance with the production of H22Y-mEGF in *P. pastoris*. We thank S. Orchard for constructing the T581A mutant and N. Hall for helpful discussions regarding the structure of the EGFR. We thank Dr. C. Arteaga for the generous gift of the C225 antibody. We are grateful to Dr. C. Cobb, Dr. J. Wilkinson, J. Songcharoen, and Dr. J. C. Whitson for assistance with fluorescence experiments, C. Alford and Dr. N. Dixit for assistance with cell viability studies, and Dr. R. A. Stein and Dr. E. J. Hustedt for helpful discussions.

REFERENCES

1. Alroy, I., and Yarden, Y. (1997) The ErbB signaling network in embryogenesis and oncogenesis: Signal diversification through combinatorial ligand−receptor interactions, *FEBS Lett. 410*, 83−86.
2. Ge, G., Wu, J., Wang, Y., and Lin, Q. (2002) Activation mechanism of solubilized epidermal growth factor receptor tyrosine kinase, *Biochem. Biophys. Res. Commun. 290*, 914−920.
3. Jorissen, R. N., Walker, F., Pouliot, N., Garrett, T. P., Ward, C. W., and Burgess, A. W. (2003) Epidermal growth factor receptor: Mechanisms of activation and signalling, *Exp. Cell Res. 284*, 31−53.
4. Arteaga, C. L. (2002) Overview of epidermal growth factor receptor biology and its role as a therapeutic target in human neoplasia, *Semin. Oncol. 29*, 3−9.
5. Rowinsky, E. K. (2004) The erbB family: Targets for therapeutic development against cancer and therapeutic strategies using monoclonal antibodies and tyrosine kinase inhibitors, *Annu. Rev. Med. 55*, 433−457.
6. Ogiso, H., Ishitani, R., Nureki, O., Fukai, S., Yamanaka, M., Kim, J. H., Saito, K., Sakamoto, A., Inoue, M., Shirouzu, M., and Yokoyama, S. (2002) Crystal structure of the complex of human epidermal growth factor and receptor extracellular domains, *Cell 110*, 775−787.
7. Garrett, T. P., McKern, N. M., Lou, M., Elleman, T. C., Adams, T. E., Lovrecz, G. O., Zhu, H. J., Walker, F., Frenkel, M. J., Hoyne, P. A., Jorissen, R. N., Nice, E. C., Burgess, A. W., and Ward, C. W. (2002) Crystal structure of a truncated epidermal growth factor receptor extracellular domain bound to transforming growth factor α, *Cell 110*, 763−773.
8. Ferguson, K. M., Berger, M. B., Mendrola, J. M., Cho, H. S., Leahy, D. J., and Lemmon, M. A. (2003) EGF activates its receptor by removing interactions that autoinhibit ectodomain dimerization, *Mol. Cell 11*, 507−517.
9. Cho, H. S., and Leahy, D. J. (2002) Structure of the extracellular region of HER3 reveals an interdomain tether, *Science 297*, 1330−1333.
10. Garrett, T. P., McKern, N. M., Lou, M., Elleman, T. C., Adams, T. E., Lovrecz, G. O., Kofler, M., Jorissen, R. N., Nice, E. C., Burgess, A. W., and Ward, C. W. (2003) The crystal structure of a truncated ErbB2 ectodomain reveals an active conformation, poised to interact with other ErbB receptors, *Mol. Cell 11*, 495−505.
11. Li, S., Schmitz, K. R., Jeffrey, P. D., Wiltzius, J. J., Kussie, P., and Ferguson, K. M. (2005) Structural basis for inhibition of the epidermal growth factor receptor by cetuximab, *Cancer Cell 7*, 301−311.
12. Burgess, A. W., Cho, H. S., Eigenbrot, C., Ferguson, K. M., Garrett, T. P., Leahy, D. J., Lemmon, M. A., Sliwkowski, M. X., Ward, C. W., and Yokoyama, S. (2003) An open-and-shut case? Recent insights into the activation of EGF/ErbB receptors, *Mol. Cell 12*, 541−552.
13. Berezov, A., Chen, J., Liu, Q., Zhang, H. T., Greene, M. I., and Murali, R. (2002) Disabling receptor ensembles with rationally designed interface peptidomimetics, *J. Biol. Chem. 277*, 28330−28339.
14. Cummings, R. D., Soderquist, A. M., and Carpenter, G. (1985) The oligosaccharide moieties of the epidermal growth factor receptor in A-431 cells. Presence of complex-type N-linked chains that contain terminal *N*-acetylgalactosamine residues, *J. Biol. Chem. 260*, 11944−11952.
15. Soderquist, A. M., and Carpenter, G. (1984) Glycosylation of the epidermal growth factor receptor in A-431 cells. The contribution of carbohydrate to receptor function, *J. Biol. Chem. 259*, 12586−12594.
16. Gamou, S., and Shimizu, N. (1988) Glycosylation of the epidermal growth factor receptor and its relationship to membrane transport and ligand binding, *J. Biochem. (Tokyo) 104*, 388−396.
17. Stroop, C. J., Weber, W., Gerwig, G. J., Nimtz, M., Kamerling, J. P., and Vliegenthart, J. F. (2000) Characterization of the carbohydrate chains of the secreted form of the human epidermal growth factor receptor, *Glycobiology 10*, 901−917.
18. Zhen, Y., Caprioli, R. M., and Staros, J. V. (2003) Characterization of glycosylation sites of the epidermal growth factor receptor, *Biochemistry 42*, 5478−5492.
19. Ullrich, A., Coussens, L., Hayflick, J. S., Dull, T. J., Gray, A., Tam, A. W., Lee, J., Yarden, Y., Libermann, T. A., Schlessinger, J., et al. (1984) Human epidermal growth factor receptor cDNA sequence and aberrant expression of the amplified gene in A431 epidermoid carcinoma cells, *Nature 309*, 418−425.
20. Sato, C., Kim, J. H., Abe, Y., Saito, K., Yokoyama, S., and Kohda, D. (2000) Characterization of the N-oligosaccharides attached to the atypical Asn-X-Cys sequence of recombinant human epidermal growth factor receptor, *J. Biochem. (Tokyo) 127*, 65−72.
21. Smith, K. D., Davies, M. J., Bailey, D., Renouf, D. V., and Hounsell, E. F. (1996) Analysis of the glycosylation patterns of the extracellular domain of the epidermal growth factor receptor expressed in Chinese hamster ovary fibroblasts, *Growth Factors 13*, 121−132.

22. Bishayee, S. (2000) Role of conformational alteration in the epidermal growth factor receptor (EGFR) function, *Biochem. Pharmacol. 60*, 1217−1223.
23. Takahashi, M., Tsuda, T., Ikeda, Y., Honke, K., and Taniguchi, N. (2004) Role of N-glycans in growth factor signaling, *Glycoconjugate J. 20*, 207−212.
24. Gamou, S., Shimagaki, M., Minoshima, S., Kobayashi, S., and Shimizu, N. (1989) Subcellular localization of the EGF receptor maturation process, *Exp. Cell Res. 183*, 197−206.
25. Helenius, A., and Aebi, M. (2004) Roles of N-linked glycans in the endoplasmic reticulum, *Annu. Rev. Biochem. 73*, 1019−1049.
26. Fernandes, H., Cohen, S., and Bishayee, S. (2001) Glycosylation-induced conformational modification positively regulates receptor−receptor association: A study with an aberrant epidermal growth factor receptor (EGFRvIII/ΔEGFR) expressed in cancer cells, *J. Biol. Chem. 276*, 5375−5383.
27. Tsuda, T., Ikeda, Y., and Taniguchi, N. (2000) The Asn-420-linked sugar chain in human epidermal growth factor receptor suppresses ligand-independent spontaneous oligomerization. Possible role of a specific sugar chain in controllable receptor activation, *J. Biol. Chem. 275*, 21988−21994.
28. Chao, G., Cochran, J. R., and Wittrup, K. D. (2004) Fine epitope mapping of anti-epidermal growth factor receptor antibodies through random mutagenesis and yeast surface display, *J. Mol. Biol. 342*, 539−550.
29. Walker, F., Orchard, S. G., Jorissen, R. N., Hall, N. E., Zhang, H. H., Hoyne, P. A., Adams, T. E., Johns, T. G., Ward, C., Garrett, T. P., Zhu, H. J., Nerrie, M., Scott, A. M., Nice, E. C., and Burgess, A. W. (2004) CR1/CR2 interactions modulate the functions of the cell surface epidermal growth factor receptor, *J. Biol. Chem. 279*, 22387−22398.
30. Stein, R. A., Wilkinson, J. C., Guyer, C. A., and Staros, J. V. (2001) An analytical approach to the measurement of equilibrium binding constants: Application to EGF binding to EGF receptors in intact cells measured by flow cytometry, *Biochemistry 40*, 6142−6154.
31. Whitson, K. B., Beechem, J. M., Beth, A. H., and Staros, J. V. (2004) Preparation and characterization of Alexa Fluor 594-labeled epidermal growth factor for fluorescence resonance energy transfer studies: Application to the epidermal growth factor receptor, *Anal. Biochem. 324*, 227−236.
32. Wilkinson, J. C., Stein, R. A., Guyer, C. A., Beechem, J. M., and Staros, J. V. (2001) Real-time kinetics of ligand/cell surface receptor interactions in living cells: Binding of epidermal growth factor to the epidermal growth factor receptor, *Biochemistry 40*, 10230−10242.
33. Johns, T. G., Adams, T. E., Cochran, J. R., Hall, N. E., Hoyne, P. A., Olsen, M. J., Kim, Y. S., Rothacker, J., Nice, E. C., Walker, F., Ritter, G., Jungbluth, A. A., Old, L. J., Ward, C. W., Burgess, A. W., Wittrup, K. D., and Scott, A. M. (2004) Identification of the epitope for the epidermal growth factor receptor-specific monoclonal antibody 806 reveals that it preferentially recognizes an untethered form of the receptor, *J. Biol. Chem. 279*, 30375−30384.
34. Wilkinson, J. C., and Staros, J. V. (2002) Effect of ErbB2 coexpression on the kinetic interactions of epidermal growth factor with its receptor in intact cells, *Biochemistry 41*, 8−14.
35. Wilkinson, J. C., Beechem, J. M., and Staros, J. V. (2002) A stopped-flow fluorescence anisotropy method for measuring hormone binding and dissociation kinetics with cell-surface receptors in living cells, *J. Recept. Signal Transduction Res. 22*, 357−371.
36. Ewald, J. A., Wilkinson, J. C., Guyer, C. A., and Staros, J. V. (2003) Ligand- and kinase activity-independent cell survival mediated by the epidermal growth factor receptor expressed in 32D cells, *Exp. Cell Res. 282*, 121−131.
37. Johns, T. G., Stockert, E., Ritter, G., Jungbluth, A. A., Huang, H. J., Cavenee, W. K., Smyth, F. E., Hall, C. M., Watson, N., Nice, E. C., Gullick, W. J., Old, L. J., Burgess, A. W., and Scott, A. M. (2002) Novel monoclonal antibody specific for the de2-7 epidermal growth factor receptor (EGFR) that also recognizes the EGFR expressed in cells containing amplification of the EGFR gene, *Int. J. Cancer 98*, 398−408.
38. Beechem, J. M. (1992) Global analysis of biochemical and biophysical data, *Methods Enzymol. 210*, 37−54.
39. Staros, J. V. (1982) *N*-Hydroxysulfosuccinimide active esters: Bis(*N*-hydroxysulfosuccinimide) esters of two dicarboxylic acids are hydrophilic, membrane-impermeant, protein cross-linkers, *Biochemistry 21*, 3950−3955.
40. Ewald, J. A., Coker, K. J., Price, J. O., Staros, J. V., and Guyer, C. A. (2001) Stimulation of mitogenic pathways through kinase-impaired mutants of the epidermal growth factor receptor, *Exp. Cell Res. 268*, 262−273.
41. MacLeod, C. L., Luk, A., Castagnola, J., Cronin, M., and Mendelsohn, J. (1986) EGF induces cell cycle arrest of A431 human epidermoid carcinoma cells, *J. Cell. Physiol. 127*, 175−182.
42. Wang, L. M., Kuo, A., Alimandi, M., Veri, M. C., Lee, C. C., Kapoor, V., Ellmore, N., Chen, X. H., and Pierce, J. H. (1998) ErbB2 expression increases the spectrum and potency of ligand-mediated signal transduction through ErbB4, *Proc. Natl. Acad. Sci. U.S.A. 95*, 6809−6814.
43. Pierce, J. H., Ruggiero, M., Fleming, T. P., Di Fiore, P. P., Greenberger, J. S., Varticovski, L., Schlessinger, J., Rovera, G., and Aaronson, S. A. (1988) Signal transduction through the EGF receptor transfected in IL-3-dependent hematopoietic cells, *Science 239*, 628−631.
44. Mattoon, D., Klein, P., Lemmon, M. A., Lax, I., and Schlessinger, J. (2004) The tethered configuration of the EGF receptor extracellular domain exerts only a limited control of receptor function, *Proc. Natl. Acad. Sci. U.S.A. 101*, 923−928.
45. Petrescu, A. J., Milac, A. L., Petrescu, S. M., Dwek, R. A., and Wormald, M. R. (2004) Statistical analysis of the protein environment of N-glycosylation sites: Implications for occupancy, structure, and folding, *Glycobiology 14*, 103−114.
46. Wormald, M. R., Petrescu, A. J., Pao, Y. L., Glithero, A., Elliott, T., and Dwek, R. A. (2002) Conformational studies of oligosaccharides and glycopeptides: Complementarity of NMR, X-ray crystallography, and molecular modelling, *Chem. Rev. 102*, 371−386.
47. Johns, T. G., Luwor, R. B., Murone, C., Walker, F., Weinstock, J., Vitali, A. A., Perera, R. M., Jungbluth, A. A., Stockert, E., Old, L. J., Nice, E. C., Burgess, A. W., and Scott, A. M. (2003) Antitumor efficacy of cytotoxic drugs and the monoclonal antibody 806 is enhanced by the EGF receptor inhibitor AG1478, *Proc. Natl. Acad. Sci. U.S.A. 100*, 15871−15876.
48. Luwor, R. B., Johns, T. G., Murone, C., Huang, H. J., Cavenee, W. K., Ritter, G., Old, L. J., Burgess, A. W., and Scott, A. M. (2001) Monoclonal antibody 806 inhibits the growth of tumor xenografts expressing either the de2-7 or amplified epidermal growth factor receptor (EGFR) but not wild-type EGFR, *Cancer Res. 61*, 5355−5361.
49. Carpenter, G., and Cohen, S. (1976) ^{125}I-labeled human epidermal growth factor. Binding, internalization, and degradation in human fibroblasts, *J. Cell Biol. 71*, 159−171.
50. King, A. C., and Cuatrecasas, P. (1982) Resolution of high and low affinity epidermal growth factor receptors. Inhibition of high affinity component by low temperature, cycloheximide, and phorbol esters, *J. Biol. Chem. 257*, 3053−3060.
51. Klein, P., Mattoon, D., Lemmon, M. A., and Schlessinger, J. (2004) A structure-based model for ligand binding and dimerization of EGF receptors, *Proc. Natl. Acad. Sci. U.S.A. 101*, 929−934.
52. Wofsy, C., Goldstein, B., Lund, K., and Wiley, H. S. (1992) Implications of epidermal growth factor (EGF) induced egf receptor aggregation, *Biophys. J. 63*, 98−110.
53. Stein, R. A., Hustedt, E. J., Staros, J. V., and Beth, A. H. (2002) Rotational dynamics of the epidermal growth factor receptor, *Biochemistry 41*, 1957−1964.
54. Elleman, T. C., Domagala, T., McKern, N. M., Nerrie, M., Lonnqvist, B., Adams, T. E., Lewis, J., Lovrecz, G. O., Hoyne, P. A., Richards, K. M., Howlett, G. J., Rothacker, J., Jorissen, R. N., Lou, M., Garrett, T. P., Burgess, A. W., Nice, E. C., and Ward, C. W. (2001) Identification of a determinant of epidermal growth factor receptor ligand-binding specificity using a truncated, high-affinity form of the ectodomain, *Biochemistry 40*, 8930−8939.
55. Lenferink, A. E., van Zoelen, E. J., van Vugt, M. J., Grothe, S., van Rotterdam, W., van De Poll, M. L., and O'Connor-McCourt, M. D. (2000) Superagonistic activation of ErbB-1 by EGF-related growth factors with enhanced association and dissociation rate constants, *J. Biol. Chem. 275*, 26748−26753.
56. Coker, K. J., Staros, J. V., and Guyer, C. A. (1994) A kinase-negative epidermal growth factor receptor that retains the capacity to stimulate DNA synthesis, *Proc. Natl. Acad. Sci. U.S.A. 91*, 6967−6971.

BI050751J